

On the PB Sudakov: NNLL coefficient, CS kernel and intrinsic-kt.

Aleksandra Lelek^{*}

*University of Antwerp,
Belgium*

E-mail: aleksandra.lelek@uantwerpen.be

The Transverse Momentum Dependent (TMD) Parton Branching (PB) method incorporates elements of TMD physics into a Monte Carlo (MC) framework to produce high-energy QCD predictions for collider processes. It derives TMDs from the PB evolution equation - solvable with MC techniques - fits them to data, and then enables their use in MC event generators for QCD predictions. In this article, we describe the relation of the PB Sudakov form factor to the Sudakov factor in the CSS formalism. We discuss both perturbative and non-perturbative components. We present recent developments to include NNLL coefficient in the PB Sudakov. We discuss the CS kernel extractions for different evolution scenarios. We remark the recent studies on intrinsic-kt vs center-of-mass (in)dependence in different approaches and their relation to the non-perturbative Sudakov.

QCD at the Extremes (QCDEX2025)
1–5 Sept 2025
Online

^{*}Speaker

Factorization and evolution of Transverse Momentum Dependent (TMD) parton distributions [1, 2] enable us to incorporate soft-gluon resummations in high energy QCD predictions for hadron collider observables, increasing the accuracy and reliability of the predictions. In this article, the Sudakov form factor of the TMD Parton Branching (PB) method [3, 4] will be discussed and its relation to the Sudakov of Collins-Soper-Sterman (CSS) [5] will be described, summarizing [6].

The soft gluon resolution scale and AO The standard PDFs are obtained from DGLAP evolution, with the soft gluon resolution scale $z_M \approx 1$. However, when one considers q_0 being the minimum transverse momentum of the emitted parton with which emitted parton can be resolved, then from the angular ordering (AO) of Catani-Marchesini-Webber, one obtains a condition on z_M , which becomes *dynamical*: $z_{\text{dyn}}(\mu') = 1 - q_0/\mu'$. The baseline collinear MC generators apply dynamic z_M in their PSs algorithms, still using PDFs with fixed $z_M \approx 1$ as an input guiding their evolution. The discrepancy between the forward evolution of the PDFs and backward evolution in the shower can affect precision of the obtained predictions [7, 8].

In the PB approach, instead of truncating the phase space at z_{dyn} , we use it as an intermediate scale to decompose the Sudakov form factor in two regions [6]: (i) perturbative (P) for $z < z_{\text{dyn}}$, which corresponds to $|q_\perp| > q_0$ and (ii) non-perturbative (NP) $z_{\text{dyn}} < z < z_M$ ($z_M = 1 - \epsilon$ with $0 \simeq \epsilon \ll 1$), for which $|q_\perp| < q_0$:

$$\begin{aligned} \Delta_a(\mu^2, \mu_0^2) &= \exp \left(- \int_{\mu_0^2}^{\mu^2} \frac{d\mu'^2}{\mu'^2} \left[\int_0^{z_{\text{dyn}}(\mu')} dz \frac{k_a(\alpha_s)}{1-z} - d_a(\alpha_s) \right] \right) \\ &\times \exp \left(- \int_{\mu_0^2}^{\mu^2} \frac{d\mu'^2}{\mu'^2} \int_{z_{\text{dyn}}(\mu')}^{z_M} dz \frac{k_a(\alpha_s)}{1-z} \right) = \Delta_a^{(\text{P})}(\mu^2, \mu_0^2, q_0) \cdot \Delta_a^{(\text{NP})}(\mu^2, \mu_0^2, \epsilon, q_0^2), \quad (1) \end{aligned}$$

see e.g. [4, 6] for the detailed explanation of notation. This modelling allows to discuss the resummation accuracy of PB and its non-perturbative component from the evolution.

Perturbative resummation After some algebraic manipulations [6], the perturbative PB Sudakov can be written as $\Delta_a^{(\text{P})}(\mu^2, q_0^2) = \exp \left(- \int_{q_0^2}^{\mu^2} \frac{dq_\perp^2}{q_\perp^2} \left[\frac{1}{2} k_a(\alpha_s) \ln \left(\frac{\mu^2}{q_\perp^2} \right) - d_a(\alpha_s) \right] \right)$ which coincides visually with the perturbative part of the Sudakov of CSS (with appropriate scale choices) in so-called CSS1 notation.

The following pattern is arising from the order by order comparison of the PB/DGLAP coefficients k_a and d_a with the perturbative coefficients A_a and B_a of the CSS Sudakov. Leading order (LO) splitting functions give the leading logarithmic (LL) accuracy via $k_a^{(0)} = A_a^{(1)}$ and the single logarithmic term of the next-to-leading logarithmic (NLL) accuracy with $d_a^{(0)} = -\frac{1}{2} B_a^{(1)}$ ¹; the next-to-leading order (NLO) splitting functions give the double logarithmic term at NLL $k_a^{(1)} = A_a^{(2)}$, and the single-log part of NNLL by the $d_a^{(1)}$ coefficient, here however the scheme dependence arising from the renormalization group equation has to be taken into account. The difference between the DGLAP $d_a^{(1)}$ and the standard CSS $B_a^{(2)}$ is $B_q^{(2)\text{DY}} - (-2) \cdot d_q^{(1)} = 16C_F\pi\beta_0(\zeta_2 - 1)$ and $B_g^{(2)\text{H}} - (-2) \cdot d_g^{(1)} = 16C_A\pi\beta_0(\zeta_2 + \frac{11}{24})$.

¹In PB, two separately evolved TMDs are matched with a matrix element to get the final cross section whereas in the CSS notation, the exponents from the evolution of each TMD are combined in one common Sudakov; this explains the difference of $\frac{1}{2}$.

With the next-to-next-to-leading order (NNLO) DGLAP splitting functions, the pattern is broken: $k_a^{(2)}$ does not correspond to the CSS double logarithmic coefficient at NNLL, $A_a^{(3)}$, what is referred to as the collinear anomaly [10]. The difference $A_a^{(3)} - k_a^{(2)} = C_a \pi \beta_0 [C_A (\frac{808}{27} - 28\zeta_3) - \frac{112}{27} N_f]$ is related to CS kernel via $A_a - k_a = -\frac{d\tilde{K}_a(b_\star, \mu_{b_\star})}{d \ln b_\star^2}$.

As proposed in [11, 12], by replacing the strong coupling by the physical (effective) soft-gluon coupling $\alpha_s^{\text{phys}} = \alpha_s (1 + \sum_{n=1}^{\infty} \mathcal{K}^{(n)} (\frac{\alpha_s}{2\pi})^n)$ the NLL and NNLL accuracy of the Sudakov form factor can be reached with a proper combination of the splitting functions. This method was implemented in the PB evolution equation [6], and NLL and NNLL solutions were obtained. The results are shown in left and middle panel of Fig. 1 for the TMDs and iTMDs obtained with the following evolution settings: 1.) NLO: NLO splitting functions + 2-loop α_s ; 2.) NLL: LO splitting functions + 2-loop $\alpha_s^{\text{NLL}} = \alpha_s (1 + \mathcal{K}^{(1)} (\frac{\alpha_s}{2\pi}))$ 3.) NNLL: NLO splitting functions + 2-loop $\alpha_s^{\text{NNLL}} = \alpha_s (1 + \mathcal{K}^{(2)} (\frac{\alpha_s}{2\pi})^2)$ ². For all curves, $z_M = 1 - 10^{-5}$ and $\alpha_s(q_\perp^2)$ is used, $q_0 = 1.0$ GeV, for $|q_\perp| < 1.0$ GeV α_s is frozen to the value $\alpha_s(q_0)$. The physical coupling has been implemented both in the Sudakov form factor as well as in the real emission probabilities to ensure momentum conservation [13]. The difference between NLO and NLL is significant both for TMDs and iTMDs, whereas the difference between the NLO and NNLL predictions is of the order of few %.

To investigate the impact of NLL and NNLL evolution on Z boson p_\perp spectrum at LHC, CASCADE3 [14] generator was used to match [16] the TMDs from Fig. 1 to the NLO matrix element generated with iTMD PB-NLO-2018-Set2 [15] with MCatNLO. From the right panel of Fig. 1 one can see that there is a large difference between the NLL and NLO results and the effect of going from NLO to NNLL is of the order of few %, visible in the lowest pt region.

Non-perturbative Sudakov In the non-perturbative region, the argument of α_s is set to $\alpha_s(q_0)$. With that, the non-perturbative PB Sudakov is

$$\ln \Delta_a^{(\text{NP})}(\mu^2, \mu_0^2, \epsilon, q_0^2) = -\frac{k_a(\alpha_s)}{2} \ln \left(\frac{\mu^2}{\mu_0^2} \right) \ln \left(\frac{q_0^2}{\epsilon^2 \mu_0 \mu} \right). \quad (2)$$

The logarithm of μ^2/μ_0^2 corresponds to the non-perturbative part of the Collins-Soper (CS) kernel.

We use the method of [17] to extract CS kernels from 5 phenomenological models differing in the amount of (soft) radiation, modelled in terms of α_s and z_M , as explained in the legend of Fig. 2. The results show sensitivity to the treatment of radiation: the model with the biggest amount of radiation (red) is linear at large b . When the soft region is limited by neglecting the non-perturbative Sudakov (i.e. dynamic z_M), the kernel becomes flatter at large b , the model with large $q_0 = 1$ GeV shows flat behaviour (purple). The model with $\alpha_s(\mu')$ has a contribution from very soft radiation ($z_M = 1 - 10^{-5}$) but different scale of the coupling leads to very different kernel shape.

The PB predictions are compared to a selection of results from the literature in the right panel of Fig. 2: phenomenological MAP22 [18], ART23 [19], SV19 [20] and lattice LPC22 [21, 22], SVZES [23], ETMC21 [24] and qTMDWF [25]. In contrary to other approaches, the PB extractions do not assume any parametrization: different slopes of the extracted curves are consequences of the

²At NNLL, the piece with soft-gluon coupling $\mathcal{K}^{(1)}$ is subtracted since it is proportional to $k_a^{(1)}$ and included via NLO splitting functions.

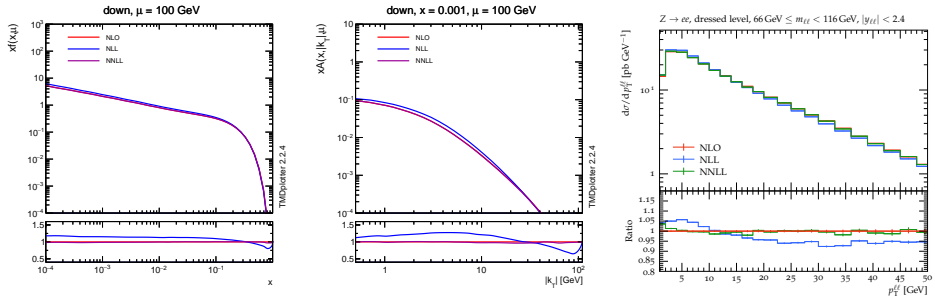


Figure 1: The PB iTMDs (left) and TMDs (middle) obtained with NLO, NLL and NNLL evolution for down quark at 100 GeV (and $x = 0.001$ for the TMD case). The prediction for Z boson p_T at 8 TeV (right) obtained with NLO ME matched to the TMDs shown in the middle plot.

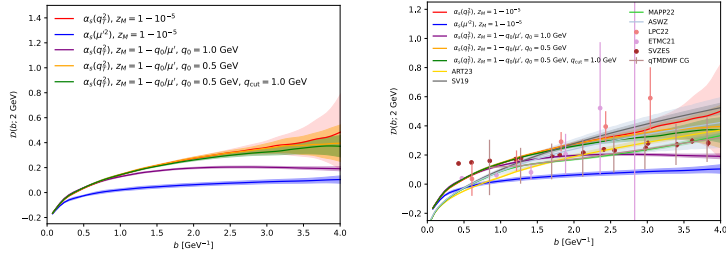


Figure 2: CS kernels extracted for different PB evolution scenarios, compared to literature examples.

different treatments of radiation. The spread of the PB results covers a significant fraction of other extractions. The result with a flattening behaviour at large b is especially interesting since most of the extractions in the literature assume a rising behaviour.

Remark on consequences of neglecting the non-perturbative Sudakov With dynamical z_M , the non-perturbative Sudakov Δ_a^{NP} is neglected. It has interesting phenomenological consequences, one of them is illustrated in Fig. 2. Another striking example is the center-of-mass energy \sqrt{s} (in)dependence of the intrinsic-kt. Standard MC generators find intrinsic-kt parameter to be strongly dependent on \sqrt{s} [26] whereas with the PB approach such a dependence is not observed [27]. The reason for that was tracked down to the treatment of soft gluons via α_s and the non-perturbative Sudakov [28, 29]. This illustrates that the known interplay of intrinsic transverse momentum with soft gluon resolution scale at the level of TMDs [27, 30] manifests itself also in physical observables and has important consequences for our predictive power.

Acknowledgements The presented results were obtained with A. Bermudez Martinez, F. Hautmann, L. Keersmaekers, M. Mendizabal Morentin, S. Taheri Monfared, A.M. van Kampen. We thank H. Jung for many discussions.

A. Lelek acknowledges funding by Research Foundation-Flanders (FWO) (1272421N, 1278325N).

References

- [1] R. Angeles-Martinez *et al.*, *Acta Phys. Polon. B* **46** (2015) no.12, 2501-2534
- [2] N. A. Abdulov *et al.*, *Eur. Phys. J. C* **81** (2021) no.8, 752
- [3] F. Hautmann *et al.*, *Phys. Lett. B* **772** (2017), 446-451
- [4] F. Hautmann *et al.*, *JHEP* **01** (2018), 070
- [5] J. Collins, “Foundations of Perturbative QCD,” Cambridge University Press, 2011,
- [6] A. B. Martinez *et al.*, *Phys. Lett. B* **868** (2025), 139762
- [7] Z. Nagy and D. E. Soper, *Phys. Rev. D* **102** (2020) no.1, 014025
- [8] S. Dooling *et al.*, *Phys. Rev. D* **87** (2013) no.9, 094009
- [9] F. Hautmann *et al.*, *Nucl. Phys. B* **949** (2019), 114795
- [10] T. Becher and M. Neubert, *Eur. Phys. J. C* **71** (2011), 1665
- [11] S. Catani *et al.*, *Eur. Phys. J. C* **79** (2019) no.8, 685
- [12] A. Banfi *et al.*, *JHEP* **01** (2019), 083
- [13] F. Hautmann *et al.*, *Phys. Lett. B* **833** (2022), 137276
- [14] S. Baranov *et al.* [CASCADE], *Eur. Phys. J. C* **81** (2021) no.5, 425
- [15] A. Bermudez Martinez *et al.*, *Phys. Rev. D* **99** (2019) no.7, 074008
- [16] A. Bermudez Martinez *et al.*, *Phys. Rev. D* **100** (2019) no.7, 074027
- [17] A. Bermudez Martinez and A. Vladimirov, *Phys. Rev. D* **106** (2022) no.9, L091501
- [18] A. Bacchetta *et al.* [MAP], *JHEP* **10** (2022), 127
- [19] V. Moos *et al.*, *JHEP* **05** (2024), 036
- [20] I. Scimemi and A. Vladimirov, *JHEP* **06** (2020), 137
- [21] M. H. Chu *et al.* [Lattice Parton (LPC)], *Phys. Rev. D* **106** (2022) no.3, 034509
- [22] Z. F. Deng *et al.*, *JHEP* **09** (2022), 046
- [23] M. Schlemmer *et al.*, *JHEP* **08** (2021), 004
- [24] Y. Li *et al.*, *Phys. Rev. Lett.* **128** (2022) no.6, 062002
- [25] D. Bollweg *et al.*, *Phys. Rev. D* **112** (2025) no.3, 034501
- [26] A. Hayrapetyan *et al.* [CMS], *Phys. Rev. D* **111** (2025) no.7, 072003

- [27] I. Bubanja *et al.*, Eur. Phys. J. C **84** (2024) no.2, 154
- [28] I. Bubanja *et al.*, Eur. Phys. J. C **85** (2025) no.3, 278
- [29] F. Hautmann *et al.*, JHEP **06** (2025), 192
- [30] S. Sadeghi Barzani, PhD thesis, Shahid Beheshti University & University of Antwerp, 2024